

pubs.acs.org/JPCA Article

# Dirac—Coulomb—Breit Molecular Mean-Field Exact-Two-Component Relativistic Equation-of-Motion Coupled-Cluster Theory

Published as part of The Journal of Physical Chemistry A virtual special issue "Gustavo Scuseria Festschrift". Tianyuan Zhang, Samragni Banerjee, Lauren N. Koulias, Edward F. Valeev, A. Eugene DePrince, III,\* and Xiaosong Li\*



Cite This: https://doi.org/10.1021/acs.jpca.3c08167



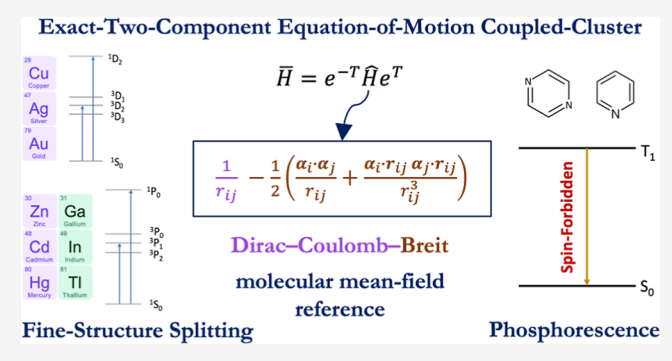
**ACCESS** 

III Metrics & More

Article Recommendations

Supporting Information

ABSTRACT: We present a relativistic equation-of-motion coupled-cluster with single and double excitation formalism within the exact two-component framework (X2C-EOM-CCSD), where both scalar relativistic effects and spin—orbit coupling are variationally included at the reference level. Three different molecular mean-field treatments of relativistic corrections, including the one-electron, Dirac—Coulomb, and Dirac—Coulomb—Breit Hamiltonian, are considered in this work. Benchmark calculations include atomic excitations and fine-structure splittings arising from spin—orbit coupling. Comparison with experimental values and relativistic time-dependent density functional theory is also carried out. The computation of the oscillator strength using the relativistic X2C-EOM-CCSD approach allows for studies phosphorescence lifetime.



of spin-orbit-driven processes, such as the spontaneous

### 1. INTRODUCTION

Excited state methods that are based on the coupled-cluster (CC) theory<sup>1–4</sup> can provide accurate descriptions of spectroscopic features, such as excitation frequencies and oscillator strengths, and are rigorously size-extensive when truncated at any excitation order. These methods include the linear response CC (LR-CC),<sup>5–12</sup> the equation-of-motion CC (EOM-CC),<sup>2,13–15</sup> and the symmetry-adapted cluster configuration interaction (SAC-CI)<sup>16</sup> formalisms. While these methods in the nonrelativistic regime are widely used and highly accurate for describing valence electron excitations of light elements, the inclusion of relativistic effects into calculations is important when dealing with core level spectroscopy, valence electron excitations of heavy elements, and spin-forbidden processes.

Relativistic effects, including scalar and spin—orbit effects, are known to cause orbital contraction, an increase in binding energy, the mixing of spin states, the modification of hybridization in the valence shell, spectral splitting, and intersystem crossing. There has been a long-standing effort to include relativistic effects in the all-electron CC framework. Early work focused on CC formalisms based on the four-component Hamiltonian and has shown great success in accurately predicting chemical properties underpinned by scalar relativity and spin—orbit coupling. General order relativistic CC implementations have also been proposed. For chemical research, electron-only relativistic theory is sufficiently

accurate, leading to the no-virtual-pair approximation in the correlation treatment. This consideration also gives rise to the use of two-component frameworks in CC calculations, in the form of Douglas–Kroll–Hess transformation-based two-component CC<sup>28,33–35</sup> and the exact-two-component (X2C) CC. Two-component approaches have the advantage of using a contracted basis in correlation calculations with reduced computational cost. The relativistic EOM-CC formalism has been developed within the X2C framework and has shown great promise in computational relativistic spectroscopies. More recently, the relativistic CC method has been implemented on a graphics processing unit (GPU), which holds potential for large-scale relativistic correlation calculations.

Two-component CC approaches usually utilize an untransformed (or bare) Coulomb term in correlation calculations, and two-electron spin—orbit effects are accounted for either by an empirical screened nuclear spin—orbit (SNSO) treatment. The mean-field or by a mean-field spin—orbit treatment. The mean-field

Received: December 14, 2023 Revised: April 8, 2024 Accepted: April 9, 2024



two-electron spin—orbit approach is very versatile and can be used either perturbatively \$45,46,49-56\$ or variationally \$36,38,41,48\$ within the CC framework, with either atomic mean-field \$39,41,42\$ or molecular mean-field formalism. \$36-38\$ Particularly, including mean-field two-electron spin—orbit at the molecular orbital (MO) level has been shown to be highly accurate in predicting relativistic molecular properties in CC and EOM-CC calculations. \$35,36,38,39,41\$ Earlier work using the molecular mean-field framework in correlated relativistic theory extended to the Dirac—Coulomb—Gaunt (DCG) Hamiltonian but did not consider excitation intensities. \$36-38\$

With the recent advancement in building the four-component Dirac-Coulomb-Breit (DCB) Hamiltonian using the Pauli quaternion basis and scalar integrals, 57-60 the computational cost of including relativistic two-electron interaction within the variational mean-field approach for obtaining the reference Slater determinant becomes affordable compared to the cost of the CC and EOM-CC correlation calculations. In this work, we report an implementation of a molecular mean-field relativistic X2C-EOM-CC approach. Three different relativistic molecular mean-field X2C approaches are investigated in this work, including the one-electron (1e-X2C), Dirac-Coulomb (DC-X2C), and DCB-X2C molecular mean-field reference. Both scalar and spin-orbit relativistic effects are included variationally at the mean-field reference level as a result of the fourcomponent self-consistent-field solution of the Dirac-Hartree-Fock equation. This work complements other relativistic EOM-CC studies using molecular mean-field two-component theory<sup>36-38</sup> by providing analysis on the use of the DCB-X2C mean-field Hamiltonian. In addition to excitation energies, expressions for computing oscillator strengths are also presented in this paper. Benchmark tests include atomic excitations to spin-orbit-coupled manifolds and excited state fine-structure splittings. A special emphasis will be placed on the photochemical properties, as exemplified by studies of the phosphorescence lifetime driven by state-to-state spin-orbit couplings.

#### 2. METHOD

**2.1.** Dirac–Coulomb–Breit Exact-Two-Component Molecular Mean-Field Reference. The exact-two-component  $(X2C)^{61-81}$  approach starts by solving the four-component Dirac equation within the restricted-kinetic-balanced condition  $^{82-84}$ 

$$\begin{pmatrix}
\mathbf{V} & \mathbf{T} \\
\mathbf{T} & \frac{1}{4c^2}\mathbf{W} - \mathbf{T}
\end{pmatrix}
\begin{pmatrix}
\mathbf{C}_{L}^{+} & \mathbf{C}_{L}^{-} \\
\mathbf{C}_{S}^{+} & \mathbf{C}_{S}^{-}
\end{pmatrix}$$

$$= \begin{pmatrix}
\mathbf{S} & \mathbf{0}_{2} \\
\mathbf{0}_{2} & \frac{1}{2c^2}\mathbf{T}
\end{pmatrix}
\begin{pmatrix}
\mathbf{C}_{L}^{+} & \mathbf{C}_{L}^{-} \\
\mathbf{C}_{S}^{+} & \mathbf{C}_{S}^{-}
\end{pmatrix}
\begin{pmatrix}
\boldsymbol{\epsilon}^{+} & \mathbf{0}_{2} \\
\mathbf{0}_{2} & \boldsymbol{\epsilon}^{-}
\end{pmatrix}$$
(1)

where c is the speed of light. V, T, and S are the two-component nonrelativistic potential energy, kinetic energy, and overlap matrices, respectively.  $W = (\sigma \cdot \mathbf{p})V(\sigma \cdot \mathbf{p})$  is the relativistic potential matrix, where  $\mathbf{p}$  is the linear momentum operator and  $\sigma$  contains Pauli spin matrices

$$\sigma_x = \begin{pmatrix} 0 & 1 \\ 1 & 0 \end{pmatrix}, \qquad \sigma_y = \begin{pmatrix} 0 & -i \\ i & 0 \end{pmatrix}, \qquad \sigma_z = \begin{pmatrix} 1 & 0 \\ 0 & -1 \end{pmatrix}$$
 (2)

Solving eq 1 gives rise to sets of positive/negative eigenvalues  $\{e^+\}$ ,  $\{e^-\}$  with corresponding MO coefficients  $(\mathbf{C}_{\mathrm{L}}^+ \mathbf{C}_{\mathrm{S}}^+)^{\mathrm{T}}$  for the positive, and  $(\mathbf{C}_{\mathrm{L}}^- \mathbf{C}_{\mathrm{S}}^-)^{\mathrm{T}}$  for the negative energy solutions.

The X2C transformation utilizes the solutions of the fourcomponent Dirac equation and "folds" the small component wave function into a pseudo-large component so that the fourcomponent Dirac equation becomes an effective twocomponent eigenfunction problem for electrons. We refer readers to ref 73 for implementation details, since the X2C transformation is a very successful and widely used technique. The four-component procedure must be carried out in an uncontracted basis to avoid variational collapse or prolapse. 85,86 After the X2C transformation, basis functions can be recontracted and used with the X2C Hamiltonian, resulting in a reference wave function with a much reduced dimensionfrom four-component to two-component and from uncontracted to contracted basis. In this work, we evaluate two types of X2C mean-field reference wave functions, as discussed in the following sections.

2.1.1. One-Electron X2C Reference. The one-electron X2C (1e-X2C) method uses solutions from the 1e Dirac equation. In this approach, 1e scalar relativistic effects and spin—orbit coupling are exactly incorporated during the transformation from a four-component to a two-component electronic structure framework. This method eliminates the necessity for a four-component self-consistent-field (SCF) procedure, making it a straightforward one-step approach, as it requires only the density-independent 1e four-component Hamiltonian.

To account for the two-electron spin—orbit coupling discrepancies, an empirical SNSO<sup>43</sup> factor is utilized to scale the 1e spin—orbit term. In the current study, we have employed the newly established row-dependent DCB-parametrized SNSO factor, which has demonstrated remarkable agreement with results from full DCB calculations. <sup>57–59</sup>

2.1.2. Dirac—Coulomb—Breit X2C Reference. In the DCB-X2C method, a two-step procedure is undertaken to transform the electron-only Hamiltonian from a four-component framework to a two-component one. In the first step, the four-component DCB equation is resolved self-consistently, incorporating operators that account for relativistic two-electron interactions. Subsequently, the X2C transformation is implemented utilizing the SCF solutions derived from the four-component Dirac equation. The DCB-X2C approach represents the exact transformation where both 1e and mean-field two-electron relativistic effects are transformed without any loss of accuracy.

The DCB operator in the Coulomb gauge includes the Coulomb, Gaunt, and gauge interactions  $^{82,83,87}\,$ 

$$V(r_{ij}) = \frac{1}{r_{ij}} - \frac{1}{2} \left( \frac{\boldsymbol{\alpha}_{i} \cdot \boldsymbol{\alpha}_{j}}{r_{ij}} + \frac{\boldsymbol{\alpha}_{i} \cdot \mathbf{r}_{ij} \boldsymbol{\alpha}_{j} \cdot \mathbf{r}_{ij}}{r_{ij}^{3}} \right),$$

$$\boldsymbol{\alpha}_{i,q} = \begin{pmatrix} \mathbf{0}_{2} & \boldsymbol{\sigma}_{q} \\ \boldsymbol{\sigma}_{q} & \mathbf{0}_{2} \end{pmatrix}, \qquad q = \{x, y, z\}$$
(3)

where  $\{i, j\}$  are electron indices and  $\mathbf{0}_2$  is the 2 × 2 zero matrix. These operators give rise to important relativistic two-electron interactions, such as spin-own-orbit, spin-other-orbit, spin-spin, and orbit-orbit terms, as well as their scalar products. Among various contributions in the DCB Hamiltonian, the DC term is the leading contribution in relativistic two-electron

Table 1. Error Analysis of X2C-EOM-CCSD Computed Excitation Energies and Fine-Structure Splitting in eV in Atomic Species and

		position MAE		splitting MAE				
	1e-X2C	DC-X2C	DCB-X2C	1e-X2C	DC-X2C	DCB-X2C		
DZP	0.137 (3.7%)	0.164 (5.1%)	0.160 (4.8%)	0.035 (10.4%)	0.022 (4.5%)	0.022 (4.6%)		
TZP	0.110 (3.0%)	0.120 (3.5%)	0.116 (3.3%)	0.029 (6.3%)	0.024 (5.1%)	0.024 (5.1%)		
QZP	0.086 (2.3%)	0.091 (2.6%)	0.088 (2.5%)	0.022 (5.0%)	0.018 (3.7%)	0.019 (3.8%)		
<sup>a</sup> Mean absolute errors (MAEs) compared with experimental values <sup>98</sup> are reported.								

VDZP VTZP VOZP VDZP VTZP VQZP VDZP VTZP VQZP 5.0 5.5 1e-X2C 1e-X2C 7.5 1e-X2C 4.0 4.5 6.5 3.0 3.5 5.5 Na, K, Rb Theoretical Absolute Peak Values (eV) Zn, Cd, Hg 2.0 2.5 4.5 Be+, Mg+, Ca+, Sr Cu<sup>+</sup>, Ag<sup>+</sup>, Au<sup>+</sup> Ga+, In+, TI+ 1.0 3.5 1.5 5.5 7.5 1.0 2.0 3.0 4.0 5.0 2.5 3.5 4.5 5.5 3.5 5.0 5.5 7.5 DC-X2C DC-X2C DC-X2C 4.0 4.5 6.5 3D 3.0 3.5 <sup>-2</sup>P<sub>3/2</sub>  $^3D_2$ 5.5  $^3D_3$ 2.0 2.5 4.5  ${}^{2}S_{1/2}$ 1.0 1.5 3.5 2.0 3.0 5.0 5.5 5.5 7.5 1.0 4.0 1.5 2.5 4.5 3.5 5.0 7.5 DCB-X2C DCB-X2C DCB-X2C 4.0 4.5 6.5 Cu Ga 3.0 3.5 Mg 5.5 Ag In Cd Ca 2.0 2.5 4.5 Au ΤI Hg 1.0 3.5 1.0 2.0 3.0 4.0 5.0 4.5 5.5 5.5 7.5 1.5 2.5 3.5

**Figure 1.** Comparison of different X2C references for the calculation of EOM-CCSD excitation energies (in eV) using different basis sets (ANO-RCC-VXZP, X = D/T/Q) in three different groups of isoelectronic systems. Computed results can be found in Table S7.

**Experimental Absolute Peak Values (eV)** 

interaction. The Breit term is the most computationally expensive and becomes important for late-row elements.

**2.2. Basis Set Recontraction.** The four-component Dirac—Hartree—Fock method requires the use of an uncontracted basis to avoid variational collapse or prolapse. Consequently, the X2C Hamiltonian is also presented on an uncontracted basis. In the two-component framework, the electronic solution has a lower bound, eliminating issues related to the small component and positronic states. This permits the adoption of a contracted basis, reducing computational expenses related to integral transformation and the number of orbitals. 88

In this work, we carry out a recontraction process for the X2C Fock matrix,  $\tilde{\mathbf{f}}^{X2C}$ , from an uncontracted to a contracted basis

$$f_{\gamma\delta}^{\rm X2C} = \sum_{\mu\nu} g_{\gamma\mu} g_{\delta\nu} \tilde{f}_{\mu\nu}^{\rm X2C} \tag{4}$$

where  $\{g\}$  is the original contraction coefficients. The basis set contraction scheme is defined as

$$\chi_{\gamma}(\mathbf{r}) = \sum_{\mu} g_{\gamma\mu} \tilde{\chi}_{\mu}(\mathbf{r}) \tag{5}$$

where  $\chi$  and  $\tilde{\chi}$  are contracted and uncontracted basis functions. **2.3. Molecular Mean-Field Equation-of-Motion Coupled-Cluster.** The X2C transformation yields a set of effective spinor MOs for electrons, which are complex-value linear combinations of atomic orbital (AO) spinors.

$$\psi_{p}^{X2C}(\mathbf{x}) = \begin{pmatrix} \phi_{p}^{\alpha}(\mathbf{r}) \\ \phi_{p}^{\beta}(\mathbf{r}) \end{pmatrix} = \begin{pmatrix} \sum_{\mu} c_{\mu p}^{\alpha} \chi_{\mu}(\mathbf{r}) \\ \sum_{\mu} c_{\mu p}^{\beta} \chi_{\mu}(\mathbf{r}) \end{pmatrix}$$
(6)

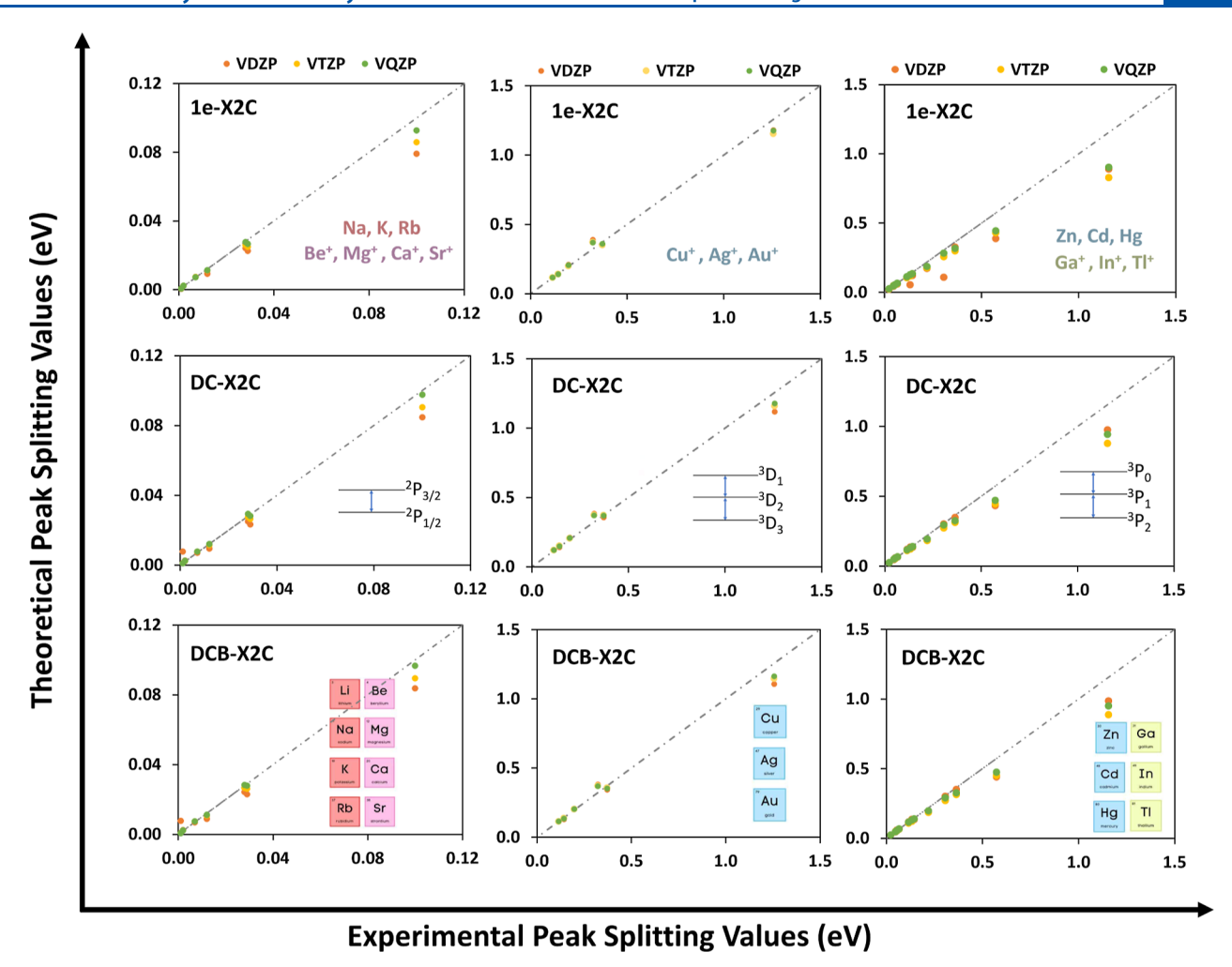


**Figure 2.** Comparison of different X2C references for the calculation of EOM-CCSD peak splittings (in eV) using different basis (ANO-RCC-VXZP, X = D/T/Q) sets in three different groups of isoelectronic systems.

where coordinate **x** includes both spatial coordinate **r** and spin coordinate  $\alpha$  or  $\beta$ .

The molecular mean-field X2C-EOM-CC methodology is formulated by using the untransformed Coulomb interaction with complex-valued X2C spinor MOs. While the formal algorithmic time complexity remains consistent with non-relativistic computations, it features a considerably larger prefactor. This increase can be attributed to the expanded dimensionality inherent in the two-component framework coupled with the necessity to employ complex arithmetic calculations. For completeness, the working expressions for computing excitation energies and oscillator strengths are included in the Supporting Information.

# 3. RESULTS AND DISCUSSION

The Kramers-unrestricted relativistic X2C-CC with single and double excitations (CCSD)<sup>89</sup> and X2C-EOM-CCSD<sup>2</sup> procedures were implemented in the Chronus Quantum software package.<sup>90</sup> In the current implementation, the evaluation of the residual equations in X2C-CCSD and the construction of sigma vectors in X2C-EOM-CCSD are powered by the TiledArray<sup>91</sup> library. The Davidson procedure, generalized for complex arithmetic, is used for iterative diagonalization of the EOM-CC Hamiltonian in order to get the low energy roots. ANO-RCC basis sets with DZP, TZP, and QZP<sup>92-97</sup> are used in the benchmark calculations. The four-component Dirac—Hartree—

Fock calculations utilized the uncontracted ANO-RCC basis. After the X2C transformation, the basis is recontracted, and the CC component of the calculation is conducted using the recontracted ANO-RCC basis.

**3.1.** Atomic Excitation Energy and Fine-Structure Splitting. In this section, we analyze various atomic excitation energies and fine-structure splittings arising from the spin—orbit coupling, which is included variationally in the X2C reference. The benchmark set includes:

- ${}^1S_0 \rightarrow {}^3D_{1,2,3}$  excitations and  ${}^3D_1 {}^3D_2$  and  ${}^3D_2 {}^3D_3$  splittings in closed-shell Cu<sup>+</sup>, Ag<sup>+</sup>, and Au<sup>+</sup> cations;
- ${}^{1}S_{0} \rightarrow {}^{3}P_{0,1,2}$  excitations and  ${}^{3}P_{0} {}^{3}P_{1}$  and  ${}^{3}P_{1} {}^{3}P_{2}$  splittings in closed-shell Zn, Cd, Hg, and their corresponding isoelectronic group 13 cations (Ga<sup>+</sup>, In<sup>+</sup>, and Tl<sup>+</sup>);
- ${}^2S_{1/2} \rightarrow {}^2P_{1/2,3/2}$  excitations and  ${}^2P_{1/2} {}^2P_{3/2}$  splitting in open-shell Na, K, Rb, and their isoelectronic group 2 cations (Be<sup>+</sup>, Mg<sup>+</sup>, Ca<sup>+</sup>, and Sr<sup>+</sup>).

All computed excitation energies and fine-structure splittings can be found in the Supporting Information. Table 1 shows the overall error analysis based on comparisons with experimental values. Figures 1 and 2 show detailed analyses for each isoelectronic group.

When looking at Table 1, we see that the X2C-EOM-CCSD computed excitation energies are in very good agreement with

the experiment with a percent error of  $\sim 2-5\%$ . The QZ basis set clearly has the best results with a MAE of 80-90 meV, compared to 130-170 and 110-120 meV for the DZ and TZ basis sets for atomic excitation energies. The same trend is observed for the calculated fine-structure splittings, although the difference is not as significant. The improvement from TZ to QZ basis is still noticeable, suggesting that basis set convergence has not been achieved yet, highlighting the need for >QZ basis for relativistic electronic structure theories.

Comparing the three different relativistic molecular meanfield references, the more accurate DC-X2C and DCB-X2C references show a marginal improvement over the 1e-X2C approach. This is understandable as the SNSO approximation used in this work is parametrized based on the DCB Hamiltonian. 44 Because the frequency-independent DCB operator provides the most accurate description of electronelectron interaction before going to a genuine relativistic quantum electrodynamics theory, the remaining computational error is most likely due to the basis set recontraction and incompleteness, the lack of higher excitations, and the absence of a correlated DCB approach, specifically the exclusion of Breit integrals in the transformation from AOs to MOs.<sup>99</sup> In this benchmark series, the difference between the DC and DCB mean-field references is relatively small. Additionally, as illustrated in Table S8 of the Supporting Information, the difference between DCG and DCB mean-field references is only in the 1-2 meV range. However, this trend may not hold for core-electron excitations as the Breit Hamiltonian becomes more important in describing core orbitals.<sup>95</sup>

Figures 1 and 2 show that the QZ basis improves the computed results for nearly all species except in the excitation energies of the Cu<sup>+</sup>, Ag<sup>+</sup>, and Au<sup>+</sup> series using the 1e-X2C meanfield reference, where the small DZ basis is more accurate. However, we emphasize that this is an example of a false positive result when an approximate relativistic Hamiltonian is used with a small basis.

Figure 1 shows that all X2C Hamiltonians underestimate the excitation energies of the coinage metal ions. For example, the MAEs for DCB-X2C-EOM-CCSD using the recontracted basis range from 0.294 eV for Cu<sup>+</sup> to 0.207 eV for Au<sup>+</sup> (Tables 2 and S7). Table S5 in the Supporting Information shows that this large error is observed across all microstates in the <sup>3</sup>D manifold. Expanding the basis set size or using an uncontracted basis (Tables 2 and S8) results in only a marginal overall

Table 2. Mean Absolute Errors (MAEs) in X2C-EOM-CCSD Computed Excitation Energies and Fine-Structure Splittings (in eV), Using the Uncontracted and Recontracted ANO-RCC-VQZP Basis Sets, 92-97 Compared with Their Experimental Values 98

atom		position Ma	AE	splitting MAE				
	1e-X2C	DC-X2C	DCB-X2C	1e-X2C	DC-X2C	DCB-X2C		
	Contracted Basis							
$Cu^+$	0.304	0.304	0.294	0.003	0.007	0.004		
$Ag^+$	0.271	0.293	0.278	0.011	0.007	0.013		
$Au^+$	0.102	0.232	0.207	0.063	0.063	0.070		
	Uncontracted Basis							
$Cu^+$	0.269	0.274	0.263	0.002	0.008	0.003		
$Ag^+$	0.289	0.298	0.283	0.010	0.007	0.013		
$Au^+$	0.170	0.189	0.164	0.039	0.042	0.053		

improvement. This observation suggests that this large error is likely due to the lack of higher excitations in CC.

Excitations in atomic species can be used to validate the computation of the oscillator strength in the Kramersunrestricted framework with relativistic operators. For atoms with the <sup>2</sup>S<sub>1/2</sub> configuration (alkali metal atoms and alkaline earth metal cations), the ground state is doubly degenerate with  $M_I = \pm \frac{1}{2}$ . The ground state reference is chosen to be the  $M_I = \frac{1}{2}$  configuration. As a result of the selection rule,  $\Delta M_I = 0$ ,  $\pm 1$ , transitions from the  $M_I = \frac{1}{2}$  ground state to the  $M_I = \pm \frac{1}{2}$ microstates of the  ${}^2P_{1/2}$  manifold are all allowed, exhibiting nonzero oscillator strengths. However, the excitation from  $M_J = \frac{1}{2}$  ground state to the  $M_J = -\frac{3}{2}$  microstate of the  $^2P_{3/2}$ manifold is forbidden (zero oscillator strengths). These characteristic excitations are correctly predicted by X2C-EOM-CC. In addition, although the calculations are done in the Kramers-unrestricted framework, time-reversal symmetries and degeneracies of excited states, e.g., 2 for the  ${}^{2}P_{1/2}$  manifold and 4 for the  ${}^{2}P_{3/2}$  manifold, are recovered to be within 1 meV in the EOM-CC approach. 100

**3.2. Basis Set Recontraction Error.** Although the four-component Dirac—Hartree—Fock mean-field procedure requires the use of an uncontracted basis, the X2C-CC part of the calculation can utilize a contracted basis. This was achieved through a basis set recontraction procedure after the X2C transformation (Section 2.2). The decreased computational cost of X2C-CC when using a contracted basis inevitably comes with a trade-off in accuracy.

Table 2 presents a comparison of excitation energies and fine-structure splittings for coinage metal cations calculated using both recontracted and uncontracted bases in the X2C-CC calculations. This comparison specifically looks at the  $^1S_0 \rightarrow ^3D_{1,2,3}$  excitations and the splittings between  $^3D_1-^3D_2$  and  $^3D_2-^3D_3$ . The table shows that the error associated with basis set recontraction is generally small, although it increases for heavier elements. The difference between recontracted and uncontracted bases for excitation energies is in the range of 5–40 meV for the DCB-X2C mean-field reference, whereas for the fine-structure splittings of excited states, it is below 17 meV. This suggests that for correlation calculations of valence electrons, employing a recontracted basis can offer a computationally efficient approach with minimal error.

Figure 2 shows that the largest absolute error in each test set is attributed to the largest splitting, which corresponds to the heaviest element and its most energetic excitation. Table S8 indicates that the error from basis set recontraction is most pronounced in the highest excited state of the heaviest element. For instance, the error in the  ${}^3D_2 - {}^3D_1$  splitting decreases from 92 to 55 meV with the use of an uncontracted basis, primarily due to the improved accuracy in the energy level of the  ${}^3D_1$  state (Table S8).

**3.3. Comparison with X2C-TDDFT.** A comparison to X2C-time-dependent density functional theory (TDDFT), 77,101 the modern day workhorse for computational spectroscopy, is a useful benchmark to show the accuracy of the X2C-EOM-CC approach. Table 3 shows a comparison of the computing excitation energies and fine-structures of the first excited state manifold (3D) of closed-shell coinage atomic cations. X2C-TDDFT calculations using the noncollinear version of the BLYP, 102,103 B3LYP, 104-106 and CAM-B3LYP 107 functionals

Table 3. Comparison of Computed Excitation Energies and Fine-Structure Splittings in Closed-Shell Transition Metal Cations Using X2C-TDDFT and X2C-EOM-CC<sup>a</sup>

	excitation			splitting			
	$^{1}S_{0} \rightarrow {}^{3}D_{3}$	$^{1}S_{0} \rightarrow {}^{3}D_{2}$	$^{1}S_{0} \rightarrow {}^{3}D_{1}$	MAE	$^{3}D_{3}-^{3}D_{2}$	$^{3}D_{2}-^{3}D_{1}$	MAE
			Cu <sup>+</sup>				
1e-X2C-TDBLYP	1.172	1.299	1.428	1.542	0.127	0.129	0.014
1e-X2C-TDB3LYP	1.827	1.955	2.091	0.884	0.128	0.136	0.010
1e-X2C-TDCAMB3LYP	1.886	2.011	2.146	0.828	0.126	0.135	0.010
1e-X2C-EOM	2.413	2.531	2.672	0.304	0.117	0.141	0.003
DC-X2C-EOM	2.407	2.529	2.678	0.304	0.121	0.149	0.007
DCB-X2C-EOM	2.426	2.541	2.677	0.294	0.115	0.136	0.004
exp.	2.719	2.833	2.975		0.114	0.143	
			$Ag^+$				
1e-X2C-TDBLYP	3.580	3.800	4.125	1.464	0.220	0.325	0.100
1e-X2C-TDB3LYP	4.056	4.277	4.613	0.795	0.221	0.336	0.03
1e-X2C-TDCAMB3LYP	4.133	4.351	4.684	0.910	0.219	0.332	0.097
1e-X2C-EOM	4.581	4.788	5.148	0.271	0.206	0.360	0.01
DC-X2C-EOM	4.555	4.764	5.134	0.293	0.209	0.370	0.007
DCB-X2C-EOM	4.578	4.783	5.137	0.278	0.205	0.355	0.013
exp.	4.856	5.052	5.423		0.196	0.372	
			$Au^+$				
1e-X2C-TDBLYP	0.917	1.368	2.508	0.900	0.451	1.140	0.122
1e-X2C-TDB3LYP	1.258	1.698	2.844	0.565	0.440	1.146	0.113
1e-X2C-TDCAMB3LYP	1.341	1.770	2.903	0.494	0.429	1.133	0.115
1e-X2C-EOM	1.757	2.127	3.304	0.102	0.370	1.177	0.063
DC-X2C-EOM	1.625	1.997	3.176	0.232	0.372	1.179	0.063
DCB-X2C-EOM	1.656	2.026	3.190	0.207	0.370	1.163	0.070
exp.	1.865	2.187	3.443		0.323	1.255	

<sup>&</sup>lt;sup>a</sup>MAEs in peak position and splitting are reported, compared with experimental values. <sup>98</sup>

Table 4. Phosphorescence Lifetimes of Various Conjugated Systems<sup>a</sup>

		· -						
		$\Delta E$ (au)	f(au)	$\tau$ (s)	experimental lifetime (s)			
Ethylene								
1e-X2C	C-TDB3LYP	0.1484	$3.26 \times 10^{-10}$	4.30	11			
1e-X2C	C-EOM	0.1626	$2.04 \times 10^{-10}$	5.71				
DC-X2	C-EOM	0.1624	$9.47 \times 10^{-11}$	12.36				
DCB-X	2C-EOM	0.1625	$1.09 \times 10^{-10}$	10.73				
			Pyridine					
1e-X2C	C-TDB3LYP	0.0731	$1.96 \times 10^{-8}$	0.30	0.24			
1e-X2C	C-EOM	0.0881	$2.55 \times 10^{-8}$	0.16				
DC-X2	C-EOM	0.0880	$3.76 \times 10^{-8}$	0.11				
DCB-X	2C-EOM	0.0880	$2.82 \times 10^{-8}$	0.14				
			Pyrazine					
1e-X2C	C-TDB3LYP	0.1115	$8.19 \times 10^{-8}$	0.030	0.02			
1e-X2C	C-EOM	0.1295	$1.25 \times 10^{-7}$	0.015				
DC-X2	C-EOM	0.1294	$1.81 \times 10^{-7}$	0.010				
DCB-X	2C-EOM	0.1294	$8.32 \times 10^{-8}$	0.022				
<sup>a</sup> Experimental data from re	fs 109-112.							

are compared to X2C-EOM-CCSD and experimental values. The ANO-RCC-QZP basis  $set^{92-94}$  is used in all calculations.

Compared to experimental values, X2C-TDDFT with a pure functional severely underestimates the excitation energies by 0.9–1.5 eV. Hybrid functionals (B3LYP and CAM-B3lYP) improve the results but still have an error in the range of 0.5–0.9 eV. The fine-structure splittings predicted by X2C-TDDFT also show errors that can be as large as 0.1 eV. These results signify the need for new exchange—correlation functionals that are optimized for relativistic electronic structures.

In contrast, X2C-EOM-CC results are in much better agreement with the experiment, significantly improving

predictions compared with X2C-TDDFT for both excitation energies and fine-structure splittings. All three X2C mean-field approaches are of a similar quality, although an outlier exists. The 1e-X2C-EOM-CC computed  $\mathrm{Au^+}$  excitation energies are in a noticeable better agreement with the experiment compared to other X2C mean-field approaches. This is likely due to fortuitous error cancellation in the approximate 1e-X2C Hamiltonian.

**3.4. Phosphorescence Lifetime.** Phosphorescence is a radiative transition between electronic states of different spin multiplicities, most often between the first excited state triplet and the ground state singlet. While excitations between the ground state and excited state singlets are spin allowed, the

transitions between triplet and singlet states are spin forbidden. These excitations occur due to spin—orbit couplings.

In this section, we calculate the phosphorescent lifetimes of various conjugated molecules as a way to benchmark X2C-EOM-CCSD computed oscillator strengths. The spontaneous phosphorescence process originates from the triplet geometry minimum. All triplet geometries were optimized using scalar-relativistic DFT with the B3LYP functional 104–106 and the cc-pVQZ 92–94,108 basis set. These geometries can be found in the Supporting Information. All EOM-CC calculations in this section were done using the ANO-RCC-VTZP 92–97 basis set. A singlet electronic reference is used in the EOM-CC calculations at the triplet geometry, and the singlet—triplet oscillator strength is computed to resolve the phosphorescence lifetime.

The phosphorescent rate of the states can be calculated using the Einstein coefficient for spontaneous emission, *A*, which is defined as (in atomic units)

$$A = \frac{1}{\tau} = \frac{4(\Delta E)^3}{3c^3} |\langle \Psi_{\rm T} | \hat{\mu} | \Psi_{\rm S} \rangle|^2$$
$$= \frac{2(\Delta E)^2 f}{c^3} \tag{7}$$

where  $\tau$  is the lifetime and  $\hat{\mu}$  is the dipole moment operator.  $\Delta E$  and  $\langle \Psi_{\rm T} | \hat{\mu} | \Psi_{\rm S} \rangle$  are the energy difference and transition dipole moment, respectively, between the triplet and singlet states.  $f = \frac{2}{3} \Delta E |\langle \Psi_{\rm T} | \hat{\mu} | \Psi_{\rm S} \rangle|^2$  is the corresponding isotropic oscillator strength.<sup>2</sup>

Table 4 presents the lifetimes of various phosphorescent molecules, as determined through X2C-EOM-CCSD calculations. This selected group of molecules, composed of carbon (C), nitrogen (N), and hydrogen (H) atoms, is characterized by weak spin—orbit couplings. As a result, these molecules exhibit long phosphorescent lifetimes, ranging from milliseconds to seconds. Predicting these extensive luminescent lifetimes accurately remains at the forefront of theoretical challenges. This is primarily because the precision of such predictions is contingent upon both the exact determination of the energy gap and the oscillator strength, factors which critically influence the observed luminescence lifetime.

Table 4 shows that the computed oscillator strengths are on the order of  $10^{-8}$ – $10^{-11}$ . Numerical tests without integral screening and tighter convergence criteria confirm that the small computed oscillator strengths are physical. Overall, the calculated lifetimes are a fairly good representation of the experimental lifetimes, being on the same order of magnitude.

The results presented in Table 4 for various X2C-EOM calculations indicate that while the calculated excitation energies are generally consistent, the oscillator strength exhibits sensitivity to how relativistic corrections are applied within the mean-field framework. Among the three X2C-EOM methods, the DCB-X2C mean-field approach produces results that are more accurate than those obtained with 1e-X2C and DC-X2C in the ethylene and pyrazine test cases. Moreover, in these test systems, the DCB-X2C-EOM method is also more accurate than the TDDFT calculations.

In the case of pyridine, all X2C-EOM approaches tend to underestimate the phosphorescence lifetime, whereas TDDFT predictions tend to overestimate it. This difference may stem from the absence of spin—orbit coupling in the geometry optimization process, a factor potentially more impactful for pyridine due to its lower symmetry compared to the other two

molecules studied. To reach a more conclusive understanding, future studies will include more test cases and incorporate X2C gradients in geometry optimization.

## 4. CONCLUSIONS AND PERSPECTIVES

In this work, we present a Kramers-unrestricted EOM-CCSD formalism, including expressions for computing oscillator strengths, within the X2C framework. Three different X2C mean-field treatments of relativistic effects, including 1e, DC, and DCB X2C mean-field references, were considered.

Benchmark calculations were conducted by using atomic excitation energies and fine-structure splittings. These calculations show that X2C-EOM-CCSD with the QZP basis and the DCB-X2C reference has the smallest error when compared with experimental results. The results are more sensitive to the choice of basis than the type of mean-field treatment of relativistic effects. Compared with relativistic X2C-TDDFT calculations, X2C-EOM-CCSD shows a significant improvement in predictions of atomic excitation energies.

The Kramers-unrestricted X2C-EOM-CCSD approach was applied to compute the phosphorescent lifetimes of small organic molecules, driven by relativistic interactions between states. Despite the long lifetimes and small oscillator strengths, X2C-EOM-CCSD exhibited excellent agreement with the experimental measurements.

This research emphasizes the necessity of advanced basis sets for relativistic electronic structure calculations. While basis sets larger than quadruple- $\zeta$  (QZ) enable a reliable extrapolation to the basis limit, accurate smaller basis sets that can accurately treat different spin—orbit components (e.g.,  $p_{1/2}$  and  $p_{3/2}$ ) are needed to facilitate more efficient relativistic calculations. The severe underestimate of atomic excitation energies in spin—orbit split manifolds predicted by DFT calculations calls for the development of new exchange—correlation functionals suitable for relativistic DFT.

Although the benchmark study indicates that the DC-X2C and DCB-X2C molecular mean-field references offer only a slight improvement over 1e-X2C for valence excitation energies, their significance could be more evident in core-electron excitations and heavy-element spectroscopies. These aspects will be explored in future research. Furthermore, benchmark calculations on phosphorescence rates suggest that DC-X2C and DCB-X2C molecular mean-field references might be essential for accurately predicting the oscillator strength.

In this work, we utilized a basis set recontraction scheme after the X2C transformation to reduce the computational cost of the CC part of the calculation. The results show that the basis set recontraction does not significantly affect the accuracy for predicting the valence excitations. It remains to be determined whether this approach is equally effective when applied to the prediction of core excitations.

## ASSOCIATED CONTENT

## Supporting Information

The Supporting Information is available free of charge at https://pubs.acs.org/doi/10.1021/acs.jpca.3c08167.

Working equations for X2C-EOM-CCSD excitation energies and oscillator strengths; excitation energies and fine-structure splittings for different groups of isoelectronic systems computed using different basis sets; and triplet geometries for phosphorescent molecules (PDF)

#### AUTHOR INFORMATION

## **Corresponding Authors**

A. Eugene DePrince, III — Department of Chemistry and Biochemistry, Florida State University, Tallahassee, Florida 32306-4390, United States; orcid.org/0000-0003-1061-2521; Email: adeprince@fsu.edu

Xiaosong Li — Department of Chemistry, University of Washington, Seattle, Washington 98195, United States; orcid.org/0000-0001-7341-6240; Email: xsli@uw.edu

#### **Authors**

Tianyuan Zhang — Department of Chemistry, University of Washington, Seattle, Washington 98195, United States

Samragni Banerjee — Department of Chemistry, University of Washington, Seattle, Washington 98195, United States

Lauren N. Koulias — Department of Chemistry, University of Washington, Seattle, Washington 98195, United States

Edward F. Valeev — Department of Chemistry, Virginia Tech, Blacksburg, Virginia 24061, United States; orcid.org/0000-0001-9923-6256

Complete contact information is available at: https://pubs.acs.org/10.1021/acs.jpca.3c08167

### **Author Contributions**

T.Z. and S.B. authors contribute equally.

#### **Notes**

The authors declare no competing financial interest.

## ACKNOWLEDGMENTS

This material is based upon work supported by the U.S. Department of Energy, Office of Science, Office of Advanced Scientific Computing Research and Office of Basic Energy Sciences, Scientific Discovery through the Advanced Computing (SciDAC) program under Award no. DE-SC0022263 (to A.E.D., E.F.V., and X.L.). S.B. acknowledges support from the Center for Many-Body Methods, Spectroscopies, and Dynamics for Molecular Polaritonic Systems (MAPOL) under subcontract from FWP 79715, which is funded as part of the Computational Chemical Sciences (CCS) program by the U.S. Department of Energy, Office of Science, Office of Basic Energy Sciences, Division of Chemical Sciences, Geosciences, and Biosciences at Pacific Northwest National Laboratory (PNNL). The development of the Chronus Quantum computational software is supported by the Office of Advanced Cyberinfrastructure, National Science Foundation (grants no. OAC-2103717 to XL, OAC-2103705 to A.E.D., and OAC-2103738 to E.F.V.). Computations were facilitated through the use of advanced computational, storage, and networking infrastructure provided by the shared facility supported by the University of Washington Molecular Engineering Materials Center (DMR-2308979) via the Hyak supercomputer system. This project used resources of the National Energy Research Scientific Computing Center, a DOE Office of Science User Facility supported by the Office of Science of the U.S. Department of Energy under Contract no. DE-AC02-05CH11231 using NERSC award ERCAP-0024336.

### REFERENCES

(1) Stanton, J. F.; Gauss, J.; Watts, J. D.; Bartlett, R. J. A Direct Product Decomposition Approach for Symmetry Exploitation in Many-Body Methods. I. Energy Calculations. *J. Chem. Phys.* **1991**, *94*, 4334–4345. (2) Stanton, J. F.; Bartlett, R. J. The Equation of Motion Coupled-Cluster Method. A Systematic Biorthogonal Approach to Molecular

- Excitation Energies, Transition Probabilities, and Excited State Properties. J. Chem. Phys. 1993, 98, 7029–7039.
- (3) Gauss, J.; Stanton, J. F. Coupled-Cluster Calculations of Nuclear Magnetic Resonance Chemical Shifts. *J. Chem. Phys.* **1995**, *103*, 3561–3577
- (4) Crawford, T. D.; Schaefer, H. F., III An Introduction to Coupled Cluster Theory for Computational Chemists. *Rev. Comput. Chem.* **2000**, *14*, 33–136.
- (5) Monkhorst, H. J. Calculation of Properties With the Coupled-Cluster Method. *Int. J. Quantum Chem.* **1977**, *12*, 421–432.
- (6) Mukherjee, D.; Mukherjee, P. K. A Response-Function Approach to the Direct Calculation of the Transition-Energy in a Multiple-Cluster Expansion Formalism. *Chem. Phys.* **1979**, *39*, 325–335.
- (7) Dalgaard, E.; Monkhorst, H. J. Some Aspects of the Time-Dependent Coupled-Cluster Approach to Dynamic Response Functions. *Phys. Rev. A* 1983, 28, 1217–1222.
- (8) Koch, H.; Jo/rgensen, P. Coupled Cluster Response Functions. *J. Chem. Phys.* **1990**, *93*, 3333–3344.
- (9) Koch, H.; Jensen, H. J. Aa.; Jo/rgensen, P.; Helgaker, T. Excitation Energies From the Coupled Cluster Singles and Doubles Linear Response Function (CCSDLR). Applications to Be,  $CH^+$ , CO, and  $H_2O$ . *J. Chem. Phys.* **1990**, 93, 3345–3350.
- (10) Koch, H.; Kobayashi, R.; Sanchez de Merás, A.; Jo/rgensen, P. Calculation of Size-Intensive Transition Moments From the Coupled Cluster Singles and Doubles Linear Response Function. *J. Chem. Phys.* **1994**, *100*, 4393–4400.
- (11) Koch, H.; Jensen, H. J. A.; Jo/rgensen, P.; Helgaker, T. Excitation Energies From the Coupled Cluster Singles and Doubles Linear Response Function (CCSDLR). Applications to Be, CH<sup>+</sup>, CO, and H2O. *J. Chem. Phys.* **1990**, 93, 3345–3350.
- (12) Pedersen, T. B.; Koch, H. Coupled Cluster Response Functions Revisited. *J. Chem. Phys.* **1997**, *106*, 8059–8072.
- (13) Emrich, K. An Extension of the Coupled Cluster Formalism to Excited States (I). *Nucl. Phys. A* **1981**, 351, 379–396.
- (14) Bartlett, R. J. Coupled-Cluster Theory and its Equation-of-Motion Extensions. *Wiley Interdiscip. Rev. Comput. Mol. Sci.* **2012**, *2*, 126–138.
- (15) Krylov, A. I. Equation-of-Motion Coupled-Cluster Methods for Open-Shell and Electronically Excited Species: The Hitchhiker's Guide to Fock Space. *Annu. Rev. Phys. Chem.* **2008**, *59*, 433–462.
- (16) Nakatsuji, H.; Ohta, K.; Hirao, K. Cluster Expansion of the Wave Function. Electron Correlations in the Ground State, Valence and Rydberg Excited States, Ionized States, and Electron Attached States of Formaldehyde by SAC and SAC-CI Theories. *J. Chem. Phys.* **1981**, 75, 2952–2958.
- (17) Pyykko, P. Relativistic Effects in Structural Chemistry. *Chem. Rev.* **1988**, *88*, 563–594.
- (18) Pyykkö, P. Relativistic Effects in Chemistry: More Common Than You Thought. *Annu. Rev. Phys. Chem.* **2012**, *63*, 45–64.
- (19) Marian, C. M. Spin-Orbit Coupling and Intersystem Crossing in Molecules. Wiley Interdiscip. Rev. Comput. Mol. Sci. 2012, 2, 187–203.
- (20) Valentine, A. J. S.; Li, X. Toward the Evaluation of Intersystem Crossing Rates with Variational Relativistic Methods. *J. Chem. Phys.* **2019**, *151*, 084107.
- (21) Valentine, A. J. S.; Li, X. Intersystem Crossings in Late-Row Elements: A Perspective. J. Phys. Chem. Lett. 2022, 13, 3039–3046.
- (22) Sekino, H.; Bartlett, R. J. Relativistic Coupled Cluster Calculations on Neutral and Highly Ionized Atoms. *Int. J. Quantum Chem.* **1990**, 38, 241–244.
- (23) Ilyabaev, E.; Kaldor, U. The Relativistic Open Shell Coupled Cluster Method: Direct Calculation of Excitation Energies in the Ne Atom. *J. Chem. Phys.* **1992**, *97*, 8455–8458.
- (24) Ilyabaev, E.; Kaldor, U. Relativistic Coupled-Cluster Calculations for Open-Shell Atoms. *Phys. Rev. A* **1993**, *47*, 137–142.
- (25) Eliav, E.; Kaldor, U.; Ishikawa, Y. Open-shell Relativistic Coupled-cluster Method with Dirac-Fock-Breit Wave Functions: Energies of the Gold Atom and its Cation. *Phys. Rev. A* **1994**, *49*, 1724–1729.

- (26) Visscher, L.; Lee, T. J.; Dyall, K. G. Formulation and Implementation of a Relativistic Unrestricted Coupled-Cluster Method Including Noniterative Connected Triples. *J. Chem. Phys.* **1996**, *105*, 8769–8776.
- (27) Eliav, E.; Kaldor, U. The Relativistic Four-component Coupled Cluster Method for Molecules: Spectroscopic Constants of SnH<sub>4</sub>. *Chem. Phys. Lett.* **1996**, 248, 405–408.
- (28) Eliav, E.; Kaldor, U.; Hess, B. A. The Relativistic Fock-space Coupled-Cluster Method for Molecules: CdH and its Ions. *J. Chem. Phys.* **1998**, *108*, 3409–3415.
- (29) Visscher, L.; Eliav, E.; Kaldor, U. Formulation and Implementation of the Relativistic Fock-space Coupled Cluster Method for Molecules. *J. Chem. Phys.* **2001**, *115*, 9720–9726.
- (30) Hirata, S.; Yanai, T.; Harrison, R. J.; Kamiya, M.; Fan, P.-D. Highorder Electron-correlation Methods with Scalar Relativistic and Spinorbit Corrections. *J. Chem. Phys.* **2007**, *126*, 024104.
- (31) Fleig, T.; Sørensen, L. K.; Olsen, J. A Relativistic 4-Component General-order Multi-reference Coupled Cluster Method: Initial Implementation and Application to HBr. *Theor. Chem. Acc.* **2007**, *118*, 347–356.
- (32) Nataraj, H. S.; Kállay, M.; Visscher, L. General Implementation of the Relativistic Coupled-cluster Method. *J. Chem. Phys.* **2010**, *133*, 234109.
- (33) Kaldor, U.; Heß, B. A. Relativistic All-electron Coupled-cluster Calculations on the Gold atom and Gold Hydride in the Framework of the Douglas-Kroll Transformation. *Chem. Phys. Lett.* **1994**, 230, 1–7.
- (34) Hess, B. A.; Kaldor, U. Relativistic All-electron Coupled-cluster Calculations on Au<sub>2</sub> in the Framework of the Douglas–Kroll Transformation. *J. Chem. Phys.* **2000**, *112*, 1809–1813.
- (35) Akinaga, Y.; Nakajima, T. Two-Component Relativistic Equation-of-Motion Coupled-Cluster Methods for Excitation Energies and Ionization Potentials of Atoms and Molecules. *J. Phys. Chem. A* **2017**, *121*, 827–835.
- (36) Sikkema, J.; Visscher, L.; Saue, T.; Iliaš, M. The Molecular Meanfield Approach for Correlated Relativistic Calculations. *J. Chem. Phys.* **2009**, *131*, 124116.
- (37) Tecmer, P.; Severo Pereira Gomes, A.; Knecht, S.; Visscher, L. Communication: Relativistic Fock-Space Coupled Cluster Study of Small Building Blocks of Larger Uranium Complexes. *J. Chem. Phys.* **2014**, *141*, 041107.
- (38) Shee, A.; Saue, T.; Visscher, L.; Severo Pereira Gomes, A. Equation-of-Motion Coupled-Cluster Theory Based on the 4-Component Dirac—Coulomb(—Gaunt) Hamiltonian. Energies for Single Electron Detachment, Attachment, and Electronically Excited States. J. Chem. Phys. 2018, 149, 174113.
- (39) Liu, J.; Shen, Y.; Asthana, A.; Cheng, L. Two-component Relativistic Coupled-cluster Methods using Mean-field Spin-orbit Integrals. *J. Chem. Phys.* **2018**, *148*, 034106.
- (40) Koulias, L. N.; Williams-Young, D. B.; Nascimento, D. R.; DePrince, A. E.; Li, X. Relativistic Real-Time Time-Dependent Equation-of-Motion Coupled-Cluster. *J. Chem. Theory Comput.* **2019**, 15, 6617–6624.
- (41) Asthana, A.; Liu, J.; Cheng, L. Exact Two-Component Equation-of-Motion Coupled-Cluster Singles and Doubles Method using Atomic Mean-Field Spin-Orbit Integrals. *J. Chem. Phys.* **2019**, *150*, 074102.
- (42) Pototschnig, J. V.; Papadopoulos, A.; Lyakh, D. I.; Repisky, M.; Halbert, L.; Severo Pereira Gomes, A.; Jensen, H. J. A.; Visscher, L. Implementation of Relativistic Coupled Cluster Theory for Massively Parallel GPU-Accelerated Computing Architectures. *J. Chem. Theory Comput.* 2021, 17, 5509–5529.
- (43) Boettger, J. C. Approximate Two-Electron Spin-Orbit Coupling Term For Density-Functional-Theory DFT Calculations Using The Douglas-Kroll-Hess Transformation. *Phys. Rev. B* **2000**, *62*, 7809–7815.
- (44) Ehrman, J.; Martinez-Baez, E.; Jenkins, A. J.; Li, X. Improving One-Electron Exact-Two-Component Relativistic Methods with the Dirac—Coulomb—Breit-Parameterized Effective Spin—Orbit Coupling. *J. Chem. Theory Comput.* **2023**, *19*, 5785—5790.

- (45) Heß, B. A.; Marian, C. M.; Wahlgren, U.; Gropen, O. A Mean-Field Spin-Orbit Method Applicable to Correlated Wavefunctions. *J. Chem. Phys.* **1996**, 251, 365–371.
- (46) Iliaš, M.; Kellö, V.; Visscher, L.; Schimmelpfennig, B. Inclusion of Mean-field Spin—orbit Effects based on All-electron Two-Component Spinors: Pilot Calculations on Atomic and Molecular Properties. *J. Chem. Phys.* **2001**, *115*, 9667—9674.
- (47) Liu, J.; Cheng, L. An Atomic Mean-Field Spin-Orbit Approach within Exact Two-Component Theory for a Non-Perturbative Treatment of Spin-Orbit Coupling. *J. Chem. Phys.* **2018**, *148*, 144108.
- (48) Knecht, S.; Repisky, M.; Jensen, H. J. Aa.; Saue, T. Exact Two-component Hamiltonians for Relativistic Quantum Chemistry: Two-electron Picture-change Corrections Made Simple. *J. Chem. Phys.* **2022**, *157*, 114106.
- (49) Klein, K.; Gauss, J. Perturbative Calculation of Spin-Orbit Splittings Using the Equation-of-Motion Ionization-Potential Coupled-Cluster Ansatz. *J. Chem. Phys.* **2008**, *129*, 194106.
- (50) Yang, D.-D.; Wang, F.; Guo, J. Equation of Motion Coupled Cluster Method for Electron Attached States with Spin-Orbit Coupling. *Chem. Phys. Lett.* **2012**, *531*, 236–241.
- (51) Tu, Z.; Wang, F.; Li, X. Equation-of-motion Coupled-Cluster Method for Ionized States with Spin-Orbit Coupling. *J. Chem. Phys.* **2012**, *136*, 174102.
- (52) Wang, Z.; Tu, Z.; Wang, F. Equation-of-Motion Coupled-Cluster Theory for Excitation Energies of Closed-Shell Systems With Spin-Orbit Coupling. *J. Chem. Theory Comput.* **2014**, *10*, 5567–5576.
- (53) Cheng, L.; Gauss, J. Perturbative Treatment of Spin-orbit Coupling within Spin-free Exact Two-component Theory. *J. Chem. Phys.* **2014**, *141*, 164107.
- (54) Epifanovsky, E.; Klein, K.; Stopkowicz, S.; Gauss, J.; Krylov, A. I. Spin-Orbit Couplings within the Equation-of-Motion Coupled-Cluster Framework: Theory, Implementation, and Benchmark Calculations. *J. Chem. Phys.* **2015**, *143*, 064102.
- (55) Cao, Z.; Li, Z.; Wang, F.; Liu, W. Combining the Spin-Separated Exact Two-Component Relativistic Hamiltonian with the Equation-of-Motion Coupled-Cluster Method for the Treatment of Spin-Orbit Splittings of Light and Heavy Elements. *Phys. Chem. Chem. Phys.* **2017**, 19, 3713–3721.
- (56) Cheng, L.; Wang, F.; Stanton, J. F.; Gauss, J. Perturbative Treatment of Spin-Orbit-Coupling within Spin-Free Exact Two-Component Theory using Equation-of-Motion Coupled-Cluster Methods. *J. Chem. Phys.* **2018**, *148*, 044108.
- (57) Sun, S.; Stetina, T. F.; Zhang, T.; Hu, H.; Valeev, E. F.; Sun, Q.; Li, X. Efficient Four-Component Dirac—Coulomb—Gaunt Hartree—Fock in the Pauli Spinor Representation. *J. Chem. Theory Comput.* **2021**, 17, 3388—3402.
- (58) Sun, S.; Ehrman, J. N.; Sun, Q.; Li, X. Efficient Evaluation of the Breit Operator in the Pauli Spinor Basis. *J. Chem. Phys.* **2022**, *157*, 064112.
- (59) Sun, S.; Ehrman, J.; Zhang, T.; Sun, Q.; Dyall, K. G.; Li, X. Scalar Breit Interaction for Molecular Calculations. *J. Chem. Phys.* **2023**, *158*, 171101
- (60) Liao, C.; Lambros, E.; Sun, Q.; Dyall, K. G.; Li, X. Exploring Locality in Molecular Dirac-Coulomb-Breit Calculations: A Perspective. J. Chem. Theory Comput. 2023, 19, 9009–9017.
- (61) Dyall, K. G. Interfacing Relativistic and Nonrelativistic Methods. I. Normalized Elimination of the Small Component in the Modified Dirac Equation. *J. Chem. Phys.* **1997**, *106*, 9618–9626.
- (62) Dyall, K. G. Interfacing Relativistic and Nonrelativistic Methods. II. Investigation of a Low-Order Approximation. *J. Chem. Phys.* **1998**, 109, 4201–4208.
- (63) Dyall, K. G.; Enevoldsen, T. Interfacing Relativistic and Nonrelativistic Methods. III. Atomic 4-Spinor Expansions and Integral Approximations. *J. Chem. Phys.* **1999**, *111*, 10000–10007.
- (64) Dyall, K. G. Interfacing Relativistic and Nonrelativistic Methods. IV. One- and Two-Electron Scalar Approximations. *J. Chem. Phys.* **2001**, *115*, 9136–9143.

- (65) Filatov, M.; Cremer, D. A New Quasi-Relativistic Approach for Density Functional Theory Based on the Normalized Elimination of the Small Component. *Chem. Phys. Lett.* **2002**, *351*, 259–266.
- (66) Kutzelnigg, W.; Liu, W. Quasirelativistic Theory Equivalent to Fully Relativistic Theory. J. Chem. Phys. 2005, 123, 241102.
- (67) Liu, W.; Peng, D. Infinite-Order Quasirelativistic Density Functional Method Based on the Exact Matrix Quasirelativistic Theory. *J. Chem. Phys.* **2006**, *125*, 044102.
- (68) Peng, D.; Liu, W.; Xiao, Y.; Cheng, L. Making Four- and Two-Component Relativistic Density Functional Methods Fully Equivalent Based on the Idea of From Atoms to Molecule. *J. Chem. Phys.* **2007**, *127*, 104106.
- (69) Ilias, M.; Saue, T. An infinite-order two-component relativistic Hamiltonian by a simple one-step transformation. *J. Chem. Phys.* **2007**, *126*, 064102.
- (70) Liu, W.; Peng, D. Exact Two-component Hamiltonians Revisited. J. Chem. Phys. 2009, 131, 031104.
- (71) Liu, W. Ideas of Relativistic Quantum Chemistry. *Mol. Phys.* **2010**, *108*, 1679–1706.
- (72) Li, Z.; Xiao, Y.; Liu, W. On the Spin Separation of Algebraic Two-Component Relativistic Hamiltonians. *J. Chem. Phys.* **2012**, *137*, 154114.
- (73) Peng, D.; Middendorf, N.; Weigend, F.; Reiher, M. An Efficient Implementation of Two-Component Relativistic Exact-Decoupling Methods for Large Molecules. *J. Chem. Phys.* **2013**, *138*, 184105.
- (74) Egidi, F.; Goings, J. J.; Frisch, M. J.; Li, X. Direct Atomic-Orbital-Based Relativistic Two-Component Linear Response Method for Calculating Excited-State Fine Structures. *J. Chem. Theory Comput.* **2016**, *12*, 3711–3718.
- (75) Goings, J. J.; Kasper, J. M.; Egidi, F.; Sun, S.; Li, X. Real Time Propagation of the Exact Two Component Time-Dependent Density Functional Theory. *J. Chem. Phys.* **2016**, *145*, 104107.
- (76) Konecny, L.; Kadek, M.; Komorovsky, S.; Malkina, O. L.; Ruud, K.; Repisky, M. Acceleration of Relativistic Electron Dynamics by Means of X2C Transformation: Application to the Calculation of Nonlinear Optical Properties. *J. Chem. Theory Comput.* **2016**, 12, 5823–5833.
- (77) Egidi, F.; Sun, S.; Goings, J. J.; Scalmani, G.; Frisch, M. J.; Li, X. Two-Component Non-Collinear Time-Dependent Spin Density Functional Theory for Excited State Calculations. *J. Chem. Theory Comput.* **2017**, *13*, 2591–2603.
- (78) Liu, J.; Cheng, L. Relativistic Coupled-Cluster and Equation-of-Motion Coupled-Cluster Methods. *Wiley Interdiscip. Rev. Comput. Mol. Sci.* **2021**, *11*, 1536.
- (79) Sharma, P.; Jenkins, A. J.; Scalmani, G.; Frisch, M. J.; Truhlar, D. G.; Gagliardi, L.; Li, X. Exact-Two-Component Multiconfiguration Pair-Density Functional Theory. *J. Chem. Theory Comput.* **2022**, *18*, 2947–2954.
- (80) Lu, L.; Hu, H.; Jenkins, A. J.; Li, X. Exact-Two-Component Relativistic Multireference Second-Order Perturbation Theory. *J. Chem. Theory Comput.* **2022**, *18*, 2983–2992.
- (81) Hoyer, C. E.; Hu, H.; Lu, L.; Knecht, S.; Li, X. Relativistic Kramers-Unrestricted Exact-Two-Component Density Matrix Renormalization Group. *J. Phys. Chem. A* **2022**, *126*, 5011–5020.
- (82) Dyall, K. G.; Fægri, K., Jr. Introduction to Relativistic Quantum Chemistry; Oxford University Press, 2007.
- (83) Reiher, M.; Wolf, A. Relativistic Quantum Chemistry, 2nd ed.; Wiley-VCH, 2015.
- (84) Liu, W. Handbook of Relativistic Quantum Chemistry; Springer-Verlag Berlin Heidelberg, 2017.
- (85) Dyall, K. G. Relativistic Double-zeta, Triple-zeta, and Quadruple-zeta Basis Sets for the 7p Elements, with Atomic and Molecular Applications. *Theor. Chem. Acc.* **2012**, *131*, 1172.
- (86) Sun, S.; Stetina, T. F.; Zhang, T.; Li, X. On the Finite Nuclear Effect and Gaussian Basis Sets for Four-Component Dirac Hartree–Fock Calculations. In *Rare Earth Elements and Actinides: Progress in Computational Science Applications*; Penchoff, D. A., Windus, T. L., Peterson, C. C., Eds.; American Chemical Society, 2021; Vol. 1388, Chapter 10, pp 207–218.

- (87) Breit, G. Dirac's Equation and the Spin-Spin Interactions of Two Electrons. *Phys. Rev.* **1932**, *39*, 616–624.
- (88) Dyall, K. G. In *Comprehensive Computational Chemistry* 1st ed.; Yáñez, M., Boyd, R. J., Eds.; Elsevier: Oxford, 2024; pp 4–34.
- (89) Purvis, G. D.; Bartlett, R. J. A Full Coupled-cluster Singles and Doubles Model: The Inclusion of Disconnected Triples. *J. Chem. Phys.* **1982**, *76*, 1910–1918.
- (90) Williams-Young, D. B.; Petrone, A.; Sun, S.; Stetina, T. F.; Lestrange, P.; Hoyer, C. E.; Nascimento, D. R.; Koulias, L.; Wildman, A.; Kasper, J.; et al. The Chronus Quantum software package. *Wiley Interdiscip. Rev. Comput. Mol. Sci.* **2020**, *10*, No. e1436.
- (91) Calvin, J. A.; Valeev, E. F. TiledArray: A General-Purpose Scalable Block-Sparse Tensor Framework, 2000. https://github.com/valeevgroup/tiledarray (accessed April 02, 2024).
- (92) Pritchard, B. P.; Altarawy, D.; Didier, B.; Gibson, T. D.; Windus, T. L. New Basis Set Exchange: An Open, Up-to-Date Resource for the Molecular Sciences Community. J. Chem. Inf. Model. 2019, 59, 4814—4820.
- (93) Feller, D. The Role of Databases in Support of Computational Chemistry Calculations. *J. Comput. Chem.* **1996**, *17*, 1571–1586.
- (94) Schuchardt, K. L.; Didier, B. T.; Elsethagen, T.; Sun, L.; Gurumoorthi, V.; Chase, J.; Li, J.; Windus, T. L. Basis Set Exchange: A Community Database for Computational Sciences. *J. Chem. Inf. Model.* **2007**, *47*, 1045–1052.
- (95) Roos, B. O.; Veryazov, V.; Widmark, P. O. Relativistic Atomic Natural Orbital Type Basis Sets for the Alkaline and Alkaline-Earth Atoms Applied to the Ground-State Potentials for the Corresponding Dimers. *Theor. Chem. Acc.* **2004**, *111*, 345–351.
- (96) Roos, B. O.; Lindh, R.; Malmqvist, P.-Å.; Veryazov, V.; Widmark, P.-O. Main Group Atoms and Dimers Studied with a New Relativistic ANO Basis Set. *J. Phys. Chem. A* **2004**, *108*, 2851–2858.
- (97) Roos, B. O.; Lindh, R.; Malmqvist, P.-Å.; Veryazov, V.; Widmark, P.-O. New Relativistic ANO Basis Sets for Transition Metal Atoms. *J. Phys. Chem. A* **2005**, *109*, 6575–6579.
- (98) Kramida, A.; Ralchenko, Y.; Reader, J.; NIST ASD Team NIST Atomic Spectra Database, Version 5.6.1, 2018; National Institute of Standards and Technology, Gaithersburg, MD. https://physics.nist.gov/asd (accessed April 02, 2024).
- (99) Hoyer, C. E.; Lu, L.; Hu, H.; Shumilov, K. D.; Sun, S.; Knecht, S.; Li, X. Correlated Dirac—Coulomb—Breit Multiconfigurational Self-Consistent-Field Methods. *J. Chem. Phys.* **2023**, *158*, 044101.
- (100) Kasper, J. M.; Jenkins, A. J.; Sun, S.; Li, X. Perspective on Kramers Symmetry Breaking and Restoration in Relativistic Electronic Structure Methods for Open-Shell Systems. *J. Chem. Phys.* **2020**, *153*, 090903
- (101) Petrone, A.; Williams-Young, D. B.; Sun, S.; Stetina, T. F.; Li, X. An Efficient Implementation of Two-Component Relativistic Density Functional Theory with Torque-Free Auxiliary Variables. *Eur. Phys. J. B* **2018**, *91*, 169.
- (102) Becke, A. D. Density-Functional Exchange-Energy Approximation with Correct Asymptotic Behavior. *Phys. Rev. A* **1988**, 38, 3098–3100.
- (103) Miehlich, B.; Savin, A.; Stoll, H.; Preuss, H. Results Obtained with the Correlation Energy Density Functionals of Becke and Lee, Yang and Parr. *Chem. Phys. Lett.* **1989**, *157*, 200–206.
- (104) Becke, A. D. Density-Functional Thermochemistry. III. The Role of Exact Exchange. *J. Chem. Phys.* **1993**, *98*, 5648–5652.
- (105) Lee, C.; Yang, W.; Parr, R. G. Development of the Colle-Salvetti Correlation-Energy Formula into a Functional of the Electron Density. *Phys. Rev. B* **1988**, *37*, 785–789.
- (106) Stephens, P. J.; Devlin, F. J.; Chabalowski, C. F.; Frisch, M. J. Ab Initio Calculation of Vibrational Absorption and Circular Dichroism Spectra Using Density Functional Force Fields. *J. Phys. Chem.* **1994**, *98*, 11623—11627.
- (107) Yanai, T.; Tew, D. P.; Handy, N. C. A New Hybrid Exchange—Correlation Functional Using the Coulomb-Attenuating Method (CAM-B3LYP). *Chem. Phys. Lett.* **2004**, 393, 51–57.

- (108) Dunning, T. H. Gaussian Basis Sets for Use in Correlated Molecular Calculations. I. The Atoms Boron Through Neon and Hydrogen. *J. Chem. Phys.* **1989**, *90*, 1007–1023.
- (109) Minaev, B. F.; Ågren, H. Spin-catalysis Phenomena. *Int. J. Quantum Chem.* **1996**, *57*, 519–532.
- (110) Sushida, K.; Fujita, M.; Takemura, T.; Baba, H. Phosphorescence and its Characteristics in Pyridine Vapor. *Chem. Phys.* **1984**, *88*, 221–228.
- (111) Goodman, L.; Kasha, M. The Observation and Assignment of the Lowest Multiplicity-Forbidden Transition in Pyrazine. *J. Mol. Spectrosc.* **1958**, *2*, 58–65.
- (112) Lahmani, F.; Frad, A.; Tramer, A. Long Fluorescence Lifetime of Pyrazine Vapors. *Chem. Phys. Lett.* **1972**, *14*, 337–341.